FLOW FIELDS GENERATED BY *CASSIOPEA* CONTRACTIONS:

THE EFFECT OF ORAL ARMS ON FEEDING FLOWS

By

ALYSSA ROSE CONNOLLY

A Thesis Submitted to the W.A. Franke Honors College

In Partial Fulfillment of the Bachelor's Degree
with Honors in

Natural Resources

THE UNIVERSITY OF ARIZONA

M A Y 2 0 2 3

Approved by:
Dr. Laura Miller
Department of Mathematics

1 Abstract

Due to unprecedented reports of invasive jellyfish following high ocean temperatures, it is becoming increasingly important to understand how their presence in new areas changes surrounding waters. *Cassiopea* is a genus of invasive jellyfish that are a model organism for studying fluid dynamics. *Cassiopea* suction to the ocean floor, using their pulsing bells and oral arms to continually drive water upwards. To model the magnitude and directionality of their feeding flows through the fluid-structure interactions of the bell and oral arms driving fluid motion, I used simulations with the Immersed Boundary Finite Element (IBFE) Method. Prior work has neglected the prominent oral arms as a modeling simplification. This work is distinct in that the oral arms are included to represent a broad range of natural morphologies. The resulting simulations produce the deformation of the jellyfish bell and resulting fluid motion over seven pulses of the jellyfish bell across five distinct, biologically relevant oral arms models. Results show that inclusion of the oral arms significantly impacts the vorticity and vertical velocity of the currents. The simulations distinctly show the three phases of jellyfish movement and produce a vertical jet. Although the vertical jet is not maintained due to the deflection of fluid by the oral arms, increased branching, decreased size, and added porosity and movement will enhance the upward flow.

2 Introduction

Current trends in ocean warming have driven many ecosystems to states of high stress and unprecedented invasions (Banha et al., 2020). While many marine species suffer from unnatural conditions, jellyfish thrive amidst weakened competition (Beziat & Kunzmann, 2022; Keable & Ahyong, 2016). One such group, the *Cassiopea* genus, is spreading rapidly from their native range. Despite their importance in nutrient mixing and stable food webs, jellyfish are known to have harmful effects in nonnative environments. Researchers around the globe are collaborating to identify the causes of these invasions and potential solutions to restoring ecosystem balance. However, there are many open research questions regarding the mechanisms and dynamics of *Cassiopea*'s dominance.

Cassiopea, commonly known as upside-down jellyfish, are aptly named for their characteristic benthic lifestyle. While most jellyfish species are known to float passively or use their powerful bells to propel themselves through the water column, *Cassiopea* spend the majority of their adult lives settled on the seafloor. With their bell suctioned to the substrate, the oral arms, highly branched appendages used for bringing food to the mouths, extend upwards towards potential prey and threats. This behavior gives an "upside-down" appearance and facilitates feeding and environmental impacts unique to the genus.

Due to the sessile nature of the *Cassiopea* lifestyle and the low flow environments in which they live, constant movement is needed to facilitate fluid and nutrient exchange. In their native environments, this mixing is critical to the ecosystem's overall health. The jellyfish rhythmically contract and relax the muscles of their bells, moving at an average rate of approximately one pulse per second (Nath et al., 2017). In depths of less than

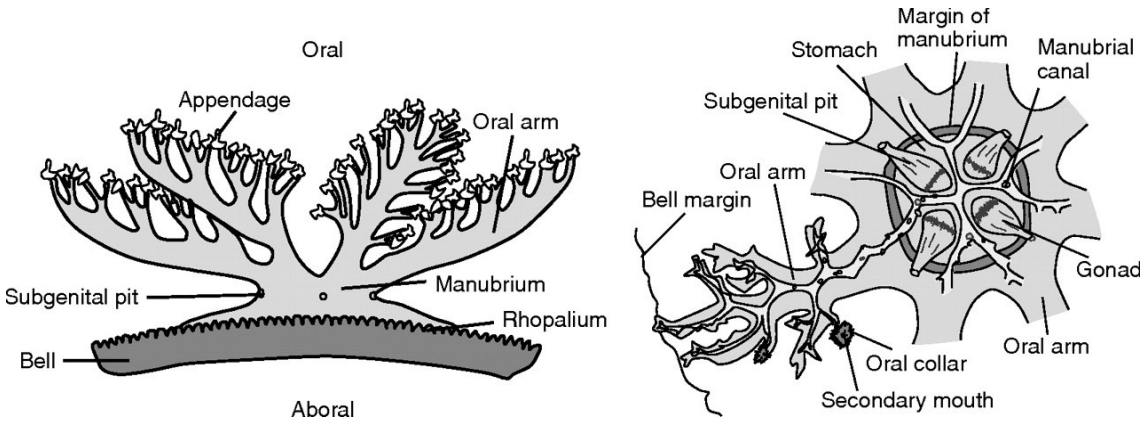

Figure 1: Main structures of a *Cassiopea xamachana* specimen (Hamlet et al., 2011 based on Hyman, 1940 drawings)

two feet, an average *Cassiopea* population can overturn the entire water column every fifteen minutes (Durieux et al., 2021). Without the interference of the swimming currents seen in pelagic jellyfish, *Cassiopea* represent a uniquely well-suited model for examining the effect of bell contractions. The three phases of the pulsing cycle (active contraction, passive expansion, and resting) create vortices that continuously drive fluid upwards (Battista et al., 2022).

Upside-down jellyfish are found in tropical and subtropical shallow waters across the globe to allow for proper light penetration for their symbiotic zooxanthellae. Dinoflagellate algae live in the endodermal cells of *Cassiopea* oral arms, providing photosynthetic products in exchange for a safe refuge (Newkirk et al., 2018). This supplemental supply of nutrients and energy contributes to *Cassiopea's* success as a highly efficient feeder, allowing them to dominate many areas they inhabit. This efficiency is due in part to *Cassiopea's* symbiosis and partially to a secreted layer of protective mucus that slows prey and contains stinging cassiosome cells (Ohdera et al., 2018). As prey are stunned by the jellyfish venom, they can be maneuvered to the mouths through the oral arms without the need for active pursuit. The oral arms play a role in both the distribution of flow fields as water is channeled through their appendages and the active movement required to finalize a successful prey capture (Hamlet et al., 2011). Despite their impact on two of *Cassiopea's* most important processes, feeding and pulsing, few studies have performed an in-depth examination of the effect of oral arms on *Cassiopea* flow. Reliable modeling of such phenomena could lead to a better understanding of how ecosystems are reduced to jellyfish-dominated shadows of their former diversity. By studying the dynamics of individual *Cassiopea*, we can lay the foundations for understanding the ecology of the genus as a whole and work towards mitigation of the group's more disastrous impacts.

As the properties of *Cassiopea* movement are still ongoing areas of study, there is a gap in the understanding of *Cassiopea*'s ecosystem dominance and range expansion. This study uses three-dimensional numerical simulations of the fluid flows produced by pulsing *Cassiopea* bells to obtain information on the velocity, direction, and range of fluid flow. Battista et al., 2022 used three-dimensional numerical simulations to model the

flow of *Cassiopea* contractions, with a special emphasis on the role of the substrate. They found that the presence of the substrate enhances the vertical jet, resulting in a stronger and faster flow. However, this model opted not to include the oral arms to isolate the effect of the substrate and simplify the mathematical model. Oral arms have been shown to significantly impact *Cassiopea's* natural flow, increasing drag and breaking up vortices (Hamlet et al., 2011). This project expands upon Battista's model to incorporate the complete jellyfish morphology with the inclusion of the oral arms. Numerical simulations using the immersed boundary method are paired with experimental dye visualizations on 3D printed models and live specimens. This project will provide imperative data on the effect of *Cassiopea*'s contractions on feeding flows, giving critical insight into the mechanisms behind the failing health of shallow-water, marine ecosystems.

3 Background

3.1 Navier-Stokes Equations

The Navier-Stokes equations, first developed in 1822 by physicists Claude-Louie Navier and George Gabriel Stokes, describe the motion of viscous fluids (NASA, n.d.). These equations are fundamental to the field of fluid dynamics and create the basis for the proposed mathematical modeling. They were introduced as an expansion on the 1775 Euler equation of motion, which was limited to non-viscous, perfect fluids. By introducing a friction component to the equation, Navier and Stokes were able to bridge the long-standing gap between experimental results and theory. These principles produce non-linear partial differential equations that revolutionized humanity's understanding of fluid mechanics in science and engineering.

The Navier-Stokes equations are as follows:

$$\rho\left(\frac{\partial u}{\partial t}+u\frac{\partial u}{\partial x}+v\frac{\partial u}{\partial y}+w\frac{\partial u}{\partial z}\right) = \rho g_x-\frac{\partial P}{\partial x}+\mu\left(\frac{\partial^2 u}{\partial x^2}+\frac{\partial^2 u}{\partial y^2}+\frac{\partial^2 u}{\partial z^2}\right) \quad (1)$$

$$\rho\left(\frac{\partial v}{\partial t}+u\frac{\partial v}{\partial x}+v\frac{\partial v}{\partial y}+w\frac{\partial v}{\partial z}\right) = \rho g_y-\frac{\partial P}{\partial y}+\mu\left(\frac{\partial^2 v}{\partial x^2}+\frac{\partial^2 v}{\partial y^2}+\frac{\partial^2 v}{\partial z^2}\right) \quad (2)$$

$$\rho\left(\frac{\partial w}{\partial t}+u\frac{\partial w}{\partial x}+v\frac{\partial w}{\partial y}+w\frac{\partial w}{\partial z}\right) = \rho g_z-\frac{\partial P}{\partial z}+\mu\left(\frac{\partial^2 w}{\partial x^2}+\frac{\partial^2 w}{\partial y^2}+\frac{\partial^2 w}{\partial z^2}\right) \quad (3)$$

in which ρ is the density of the fluid, u, v, and w are the velocity components in the x, y, and z directions respectively, t is time, g is the gravitational acceleration in the specified direction, P is pressure, and μ is the dynamic viscosity of the fluid.

In simplistic terms, the Navier-Stokes equations demonstrate that mass times acceleration is equal to the the sum of forces (including gravity, pressure differences, and viscous dissipation). Solutions are derived from Newton's second law of motion, which states that the change in motion of an object is directly proportional to the force exerted on an object. This is commonly represented as $F = ma$ where F is equal to force, m is equal to mass, and a is equal to acceleration. The solutions result in a vector field of flow velocity, describing the direction and magnitude of the fluid velocity at a point in three-dimensional space and time.

3.2 Immersed Boundary Method

To simulate the fluid dynamics caused by structure deformations, this project design uses the immersed boundary method. The immersed boundary method, first developed in 1972 by Charles Peskin to model cardiac flow, solves the Navier-Stokes equations coupled to an elastic, incompressible structure in a viscous, incompressible fluid (Peskin 2002). The fluid is comprised of millions of molecules, all of which experience different velocities and directional effects. To individually track each molecule would be an impractical and wasteful allocation of time and resources. Instead, the fluid is treated as a continuous field that deforms as a whole across time, eliminating the need for tedious particle tracking. The Navier-Stokes equations are written in an Eulerian framework and solved on a fixed Cartesian grid. The elasticity equations used for the immersed boundary method are written in a Lagrangian framework and solved on a curvilinear mesh. Eularian points are used to track the fluctuations of the fluid field, in this case ocean water, while discretized Lagrangian structures are used to describe the precise movements of the bell (Peskin, 2002). The combination of approaches prevents the flow fields from conforming to the jellyfish geometry without sacrificing the precision needed to track the movement of the bell and oral arms. Other methods exist for modeling such phenomena, but the immersed boundary method was designed specifically for biological systems. Due to the complexities inherent in the interaction between fluids and flexible materials, we believe the immersed boundary method is the proper context for examining problems of this nature. This method is further refined with the immersed boundary finite element method (IBFE), which employs the principles of classical immersed boundary modeling with improved stability (Griffith, 2017).

4 Methods

To incorporate the oral arms into the original model (Battista et al., 2022), I created twenty-one three-dimensional models of *Cassiopea* oral arms. The models were constructed from sourced field and lab photographs of *Cassiopea*, ranging across *C. andromeda*, *C. frondosa*, *C. xamachana*, *C. ndrosia*, and unspecified *Cassiopea sp.* These canvases demonstrate a variance in morphologies representative of *Cassiopea*'s natural heterogeneity. It was critical to incorporate a wide range of oral arm morphologies, as species and individuals can have significantly different densities and sizes of oral arms. Of the twenty-one unique morphologies, three categories of variation were determined: level of branching, size, and positioning. Five models were selected which represented the extremes of smooth and highly branched appendages, oral arm length relative to the bell margin, and symmetrical and oblong positioning. Variations in these factors could cause changes in the produced flow fields as water is pushed upwards by the bell and channeled through the oral arm appendages.

The oral arms models were outlined in Autodesk Fusion 360 and extruded to a three-dimensional model. The size of the models were proportionally adjusted to a 5 cm bell diameter (Battista et al., 2022) and a 0.4 cm ± 0.1 cm thickness (based on averages calculated from n=10 photographed specimens). Observations of field photographs sug-

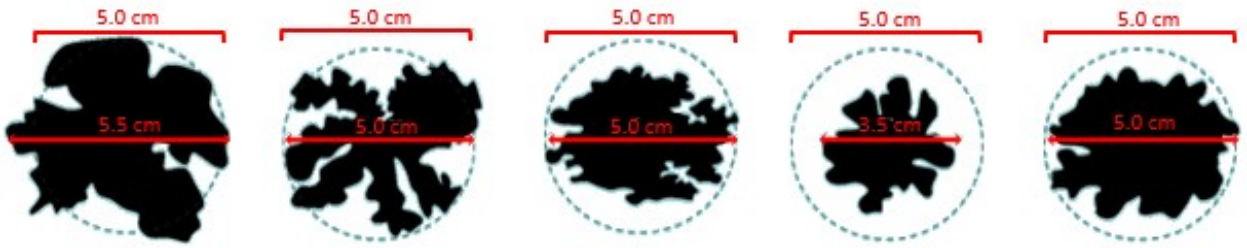

Figure 2: Top view of five oral arms models with size reference against 5 cm bell.

gest that most oral arm lengths are approximately equal to the bell radius (2.5 cm when scaled), but morphological differences are also be reflected in the length.

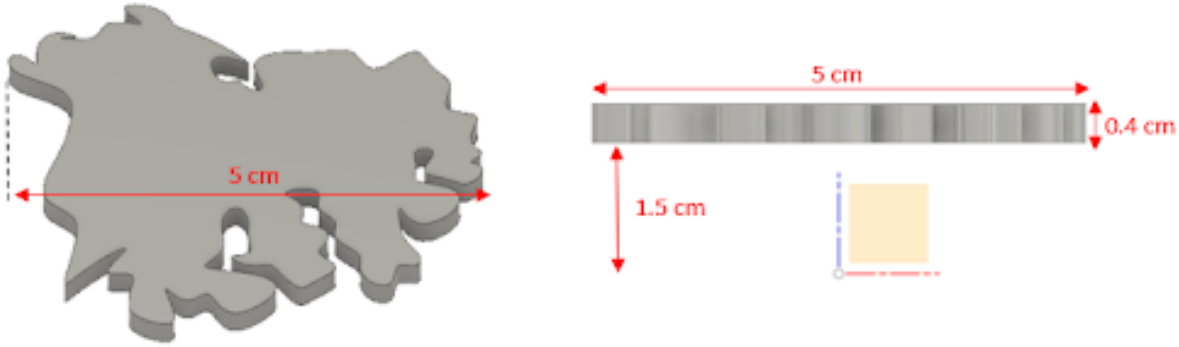

[h]

Figure 3: Top view (left) and side view (right) of *Cassiopea andromeda* model. The right figure shows a 1.5 cm vertical shift to allow for placement of the bell model underneath.

Dye visualizations were conducted in a closed tank system to confirm the significance of oral arms geometry on flow vortices and drag (Vogel & LaBarbera, 1978). The oral arms models were 3D printed with PLA filament to allow for experimentation. Clamps were used to suspend the models upright in a 102 cm x 11 cm x 12 cm plexiglass flow tank under ultraviolet (UV) light. The models were submerged in approximately 10 cm of water and results were recorded for image analysis. A current was introduced with a 2 cm/s inlet velocity on the left side of the tank, flowing against the underside of the oral arms in the direction of natural, bell-generated flow. Under low light conditions, fluorescein dye was pipetted along the underside and top face to observe contrasting dynamics in the wake. The UV light illuminated the dye to allow for clear visualization of potential flow disruptions, vortex formation, and boundary layer separation.

To be incorporated in the fluid simulations, the five oral arms models were meshed with Coreform Cubit using a 0.0005 m hex mesh. Due to the complexities inherent in the primary and secondary oral arm geometries as well as the level of refinement needed for the simulations, the software was unable to mesh the entire model as a whole. Using the webcut feature, the models were sectioned into two to four segments, allowing for proper processing under the Coreform Cubit algorithm. The sections were merged

through the imprint tool to reform a single mesh and exported to an exodus file.

Numerical simulations were run using Immersed Boundary Adaptive Mesh Refinement (IBAMR), a C++ framework for utilizing the immersed boundary finite element method in modeling viscous flow (Griffith, 2017). Taking advantage of the High Performance Computing (HPC) capabilities of this software, the jellyfish meshes were added to the bell mesh from Battista et al., 2022. Simulations took approximately half a day of computing time. When completed, the resulting viz_IB3d file was downloaded to the VisIt 3.2.2 program (Childs, 2012). This program visualizes the results, showing velocity vectors and magnitude color-mapping in time with the bell contractions.

5 Results

Results of the dye visualizations showed a distinct transition from laminar to turbulent flow upon contact with the oral arms. Figure 4 shows differences in the produced flow fields in response to variances in the oral arms. We found that the level of branching and smoothness of an area had significant impacts on the produced vortices. Figure 4a shows flow over an irregularly branched area of the model. Several short secondary appendages extend from the side of the model, resulting in a series of small, unconnected vortices. This was common in models of this nature, where highly branched areas would produce a rapid succession of individual swirls. Figure 4b demonstrates the pattern of flow seen as dye is channeled through a smoother hole formed by an extended secondary appendage. The flow did remain connected for several centimeters past the point of contact with the oral arms and produced distinct, larger vortices. These vortices were far more irregular in nature, but the smoothness of the channel prevented any major breakage in the flow. This was also seen in other models where clearly defined branching between individual oral arms created sharp, smooth channels. In figure 4c, the element of smoothness is expanded upon in a nearly linear potion of the model. This flat surface produced a vortex that was uniform in shape and followed nearly two centimeters of laminar flow. The simplified geometry led to a clear reduction in fluid disturbance. These results imply that the size and shape of *Cassiopea* oral arms is a significant driver in vortex formation, which will impact the magnitude and spread of fluid deformation.

The IBAMR simulations produced a complete model of the jellyfish morphology, and incorporated the oral arms with the bell model and motion from Battista et al., 2022. VisIt 3.2.2 visualizations successfully showed the contractions of the bell and corresponding fluid movement. Vertical velocity was plotted on a slice through the center of the jellyfish model along with the vectors. The three phases of jellyfish movement (active contraction, passive expansion, and resting) were distinct in their presence and fluid impacts. The highest magnitude of upward flow was recorded during the height of the contraction. The greatest concentration of vortex formation occurred at the edges of the oral arms layer as the fluid was funneled through the frills of the appendages. All five geometries represented by the models displayed distinct phases, although the magnitude of vertical jet produced varied according to shape. The greatest vertical jet was seen in the model with the most highly branched appendages (represented in figure 5a).

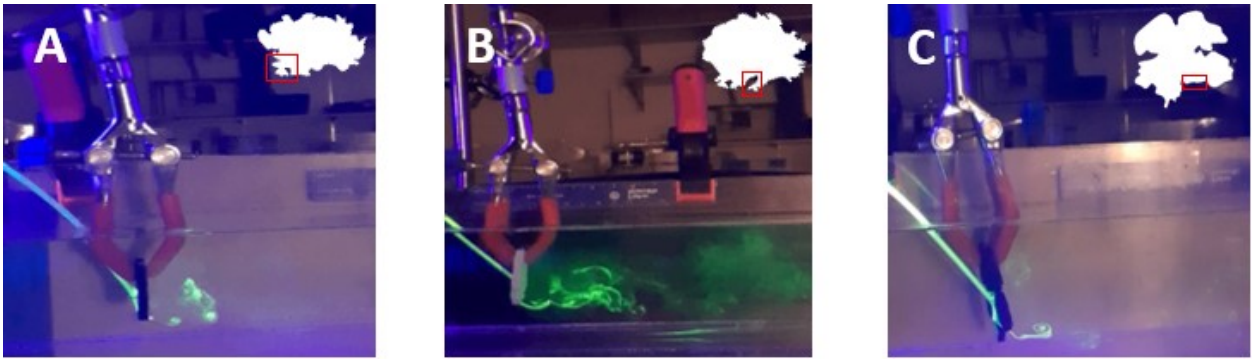

Figure 4: Fluorescein dye visualizations with 3D printed oral arms models. Different flow patterns can be seen with varying oral arms shapes (model shape is included in upper right corner with red box highlighting the area where flow is travelling over).

Models with smaller radii (such as figure 5b) maintained some upward flow around the edges of the oral arms layer, while the largest model (figure 5c) had the least amount of maintained upward flow.

The simulation data was queried to map the average vertical velocity over time (as seen in figure 6). Values greater than zero indicate that the majority of the produced flow fields are moving upward, while a value of less than zero represents a majority of downward flow. The simulation ran for seven pulses to achieve a periodic steady state and capture the best representation of flow relative to constant movement. The vertical velocity increased in magnitude for five pulses before achieving a steady distribution. Within this distribution, the active contraction, passive expansion, and resting phases were once again distinctly visible, with areas of high upward movement corresponding to contraction, downward movement corresponding to expansion, and residual effects seen in the resting phase.

6 Discussion

The presence of *Cassiopea's* three stages of locomotion in both the simulation and vertical velocity plots indicates the simulations successfully captured the dynamics of fluid movement in response to the contraction of the bell. Clear vortices and turbulent flow were produced that remain consistent with observations of live specimens and results from the fluorescein dye visualization experiments.

An upward jet is produced in all simulations and visible in the vertical velocity analysis. However, the vertical jet dynamics do not fully reflect what is seen in live *Cassiopea*. While vector analysis does indicate maintained upward flow, visualization of the vertical velocity fields does not show the presence of a significant upward jet outside of the active contraction phase. Furthermore, the vertical jet is focused on the edges of the oral arms layers instead of establishing a consistent flow directly above the jellyfish body. This is likely due to the oral arms deflecting the fluid as it is pushed through them. While oral arms do naturally interrupt the flow fields, the solid nature of the model

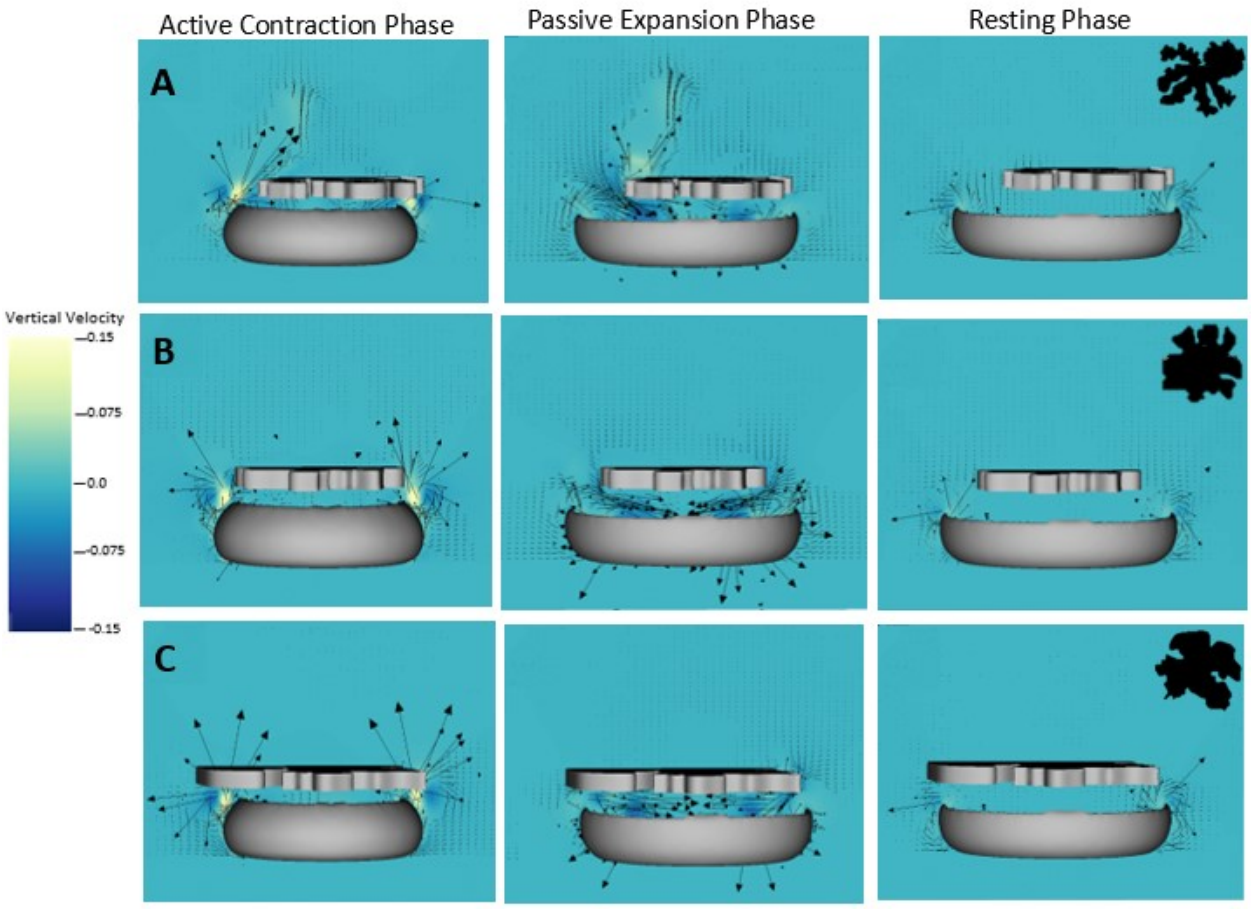

Figure 5: Results of IBAMR simulations for three oral arms models with color plot showing vertical velocity and arrows showing directionality and magnitude of vectors. Top view of oral arms included in top-right corner for reference (not to scale).

disrupts more flow than would occur in the flexible, highly branched appendages. Water is unable to move through the small gaps between secondary appendages to contribute to the vertical jet. As such, the force of the vertical jet is not powerful enough to be maintained against the downward movement from the bell's expansion. As seen in figure 5a, the only model with a significant vertical jet maintained throughout expansion was the model with the highest degree of branching. Figure 5b also has some vertical movement around the edges of the bell, due to the reduced radius of the oral arms allowing flow to escape. When the oral arms extend past the margin of the bell, flow is unable to significantly move past the oral arms. The vertical velocity plot (figure 6) shows the majority of the movement in the expansion phase is downward towards the bell. After achieving the periodic steady state, the resting phase remains approximately neutral. This once again indicates that a significant upward jet is not maintained. However, the presence of the jet in figure 5a and 5b indicates that allowing the fluid to flow through the oral arms, whether through increased branching or shorter appendages, does allow the simulation to successfully produce the maintained jet. Further enhance-

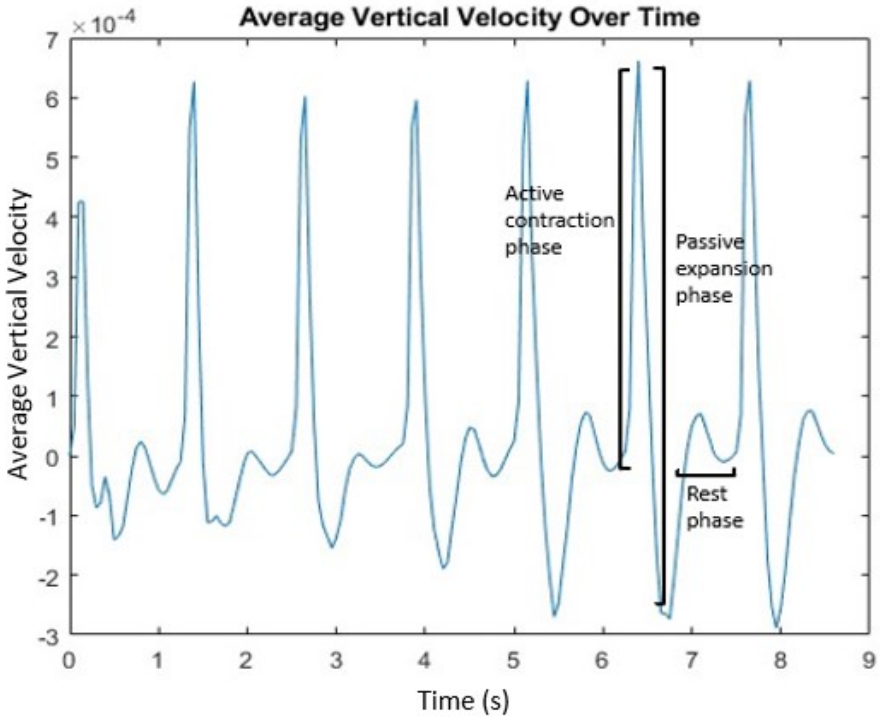

Figure 6: Plot of average vertical velocity over time for IBAMR simulation. Active contraction phase, passive expansion phase, and resting phase are distinctly represented.

ment of these principles should show the desired results.

7 Further Research

7.1 Incorporating Biological Complexity

Moving forward, the simulations should be further refined to reflect natural *Cassiopea* conditions. Although the current model is a viable starting point, real oral arms do not function as a solid disk. By making the oral arms models porous, we can simulate a more accurate depiction of flow fields. Another proposed change is to add flexibility to the oral arms in the IBFE software. As *Cassiopea* contract their bells, the oral arms naturally shift in response to the structure and fluid deformation. There is also room to explore active movement associated with feeding.

7.2 Mucus

Due to the thickness and viscosity differences between *Cassiopea*'s mucus cloud and saltwater, different areas of fluid should exhibit contrasting properties. This will affect the deformation, velocity, and spread of fluid effects. The current models simulate conditions in salt water habitats, but neglect the mucus component. As mucus dynamics are key to understanding the mechanisms behind *Cassiopea* invasions, this element is

critical to a complete understanding of *Cassiopea's* ecological impacts. Differences between mucus and water can be considered using various models of non-Newtonian fluids. Through examining past literature and observing live specimens, non-Newtonian fluid models can be developed based on the conditions seen in natural *Cassiopea* environments.

7.3 Live Specimens

Once further biological refinement and fluid properties are incorporated, the simulations can be compared to flow experimentation with live specimens. Specimens would be housed in-lab in a large saltwater tank with sufficient filtration and circulation. After allowing the *Cassiopea* to settle into their new environment, we would use dye visualisations similar in principle to the 3D model experiments. *Cassiopea* specimens would be placed in a 102cm x 11cm x 12cm plexiglass flow tank with approximately 10 cm of saltwater. Dye would be pipetted into the system to observe the flow patterns created by bell contractions. These experiments would also be paired with Particle Image Velocimetry (PIV), in which lasers illuminate tracking particles in the fluid to capture images of precise fluid movement. These results will help verify the precision of numerical simulations and allow insight into the natural patterns of *Cassiopea* bell and oral arm movement.

8 Appendix

In addition to this thesis, I have created a scientific poster in summary of the project. It can be accessed via Google drive at this link or the following url: https://docs.google.com/presentation/d/1BRlN66PSY8MMNJ9opPcgqSelDWajozZ5/edit?usp=sharing&ouid=110402037311215404277&rtpof=true&sd=true

References

[1] Thomás Banha, Miguel Mies, Arthur Güth, Christopher Pomory, and Paulo Sumida. Juvenile cassiopea andromeda medusae are resistant to multiple thermal stress events. *Marine Biology*, 167:173, 11 2020.

[2] Nicholas Battista, Manikantam G Gaddam, Christina L Hamlet, Alexander Peter Hoover, Laura Ann Miller, and Arvind Santhanakrishnan. The presence of a substrate strengthens the jet generated by upside down jellyfish. *Frontiers in Marine Science*, page 582, 2022.

[3] Pauline Béziat and Andreas Kunzmann. Under pressure: Cassiopea andromeda jellyfish exposed to increasing water temperature or lead, cadmium and anthropogenic gadolinium contamination. *Marine Biology Research*, 0(0):1–16, 2022.

[4] Hank Childs, Eric Brugger, Brad Whitlock, Jeremy Meredith, Sean Ahern, David Pugmire, Kathleen Biagas, Mark C. Miller, Cyrus Harrison, Gunther H. Weber, Hari Krishnan, Thomas Fogal, Allen Sanderson, Christoph Garth, E. Wes Bethel, David Camp, Oliver Rubel, Marc Durant, Jean M. Favre, and Paul Navratil. VisIt: An End-User Tool For Visualizing and Analyzing Very Large Data, October 2012.

[5] Boyce E Griffith and Xiaoyu Luo. Hybrid finite difference/finite element immersed boundary method. *International journal for numerical methods in biomedical engineering*, 33(12):e2888, 2017.

[6] Christina Hamlet, Arvind Santhanakrishnan, and Laura A Miller. A numerical study of the effects of bell pulsation dynamics and oral arms on the exchange currents generated by the upside-down jellyfish cassiopea xamachana. *Journal of Experimental Biology*, 214(11):1911–1921, 2011.

[7] CL Hamlet and LA Miller. Effects of grouping behavior, pulse timing, and organism size on fluid flow around the upside-down jellyfish, cassiopea xamachana. *Contemporary Mathematics*, 628:173, 2014.

[8] Libbie Henrietta Hyman. *The invertebrates: protozoa*. McGraw-Hill Book Company, 1940.

[9] Carin Jantzen, Christian Wild, Mohammed Rasheed, Mohammed El-Zibdah, and Claudio Richter. Enhanced pore-water nutrient fluxes by the upside-down jellyfish cassiopea sp. in a red sea coral reef. *Marine Ecology Progress Series*, 411:117–125, 2010.

[10] Krishan D Karunarathne, Shanika M Liyanaarachchi, and MDST De Croos. First record of upside-down jellyfish cassiopea andromeda (forskål, 1775)(cnidaria: Scyphozoa: Rhizostomeae: Cassiopeidae) from sri lanka. *Sri Lanka Journal of Aquatic Sciences*, 25(2):57–65, 2020.

[11] Stephen J Keable and Shane T Ahyong. First records of the invasive "upside-down jellyfish", cassiopea (cnidaria: Scyphozoa: Rhizostomeae: Cassiopeidae), from coastal lakes of new south wales, australia. *Records of the Australian Museum*, 68(1):23–30, 2016.

[12] NASA. Navier-stokes equations 3 dimesional unsteady. https://www.grc.nasa.gov/www/k-12/airplane/nseqs.html.

[13] Casandra R Newkirk, Thomas K Frazer, and Mark Q Martindale. Acquisition and proliferation of algal symbionts in bleached polyps of the upside-down jellyfish, cassiopea xamachana. *Journal of Experimental Marine Biology and Ecology*, 508:44–51, 2018.

[14] Aki H Ohdera, Michael J Abrams, Cheryl L Ames, David M Baker, Luis P Suescún-Bolívar, Allen G Collins, Christopher J Freeman, Edgar Gamero-Mora, Tamar L Goulet, Dietrich K Hofmann, et al. Upside-down but headed in the right direction: review of the highly versatile cassiopea xamachana system. *Frontiers in Ecology and Evolution*, page 35, 2018.

[15] Claire E Rowe, Will F Figueira, Brendan P Kelaher, Anna Giles, Lea T Mamo, Shane T Ahyong, and Stephen J Keable. Evaluating the effectiveness of drones for quantifying invasive upside-down jellyfish (cassiopea sp.) in lake macquarie, australia. *Plos one*, 17(1):e0262721, 2022.

[16] Patrick J Schembri, Alan Deidun, and Patrick J Vella. First record of cassiopea andromeda (scyphozoa: Rhizostomeae: Cassiopeidae) from the central mediterranean sea. *Marine Biodiversity Records*, 3, 2010.

[17] Mark Schrope. Attack of the blobs: jellyfish will bloom as ocean health declines, warn biologists. are they already taking over? *Nature*, 482(7383):20–22, 2012.

[18] Sergio N Stampar, Edgar Gamero-Mora, Maximiliano M Maronna, Juliano M Fritscher, Bruno SP Oliveira, Cláudio LS Sampaio, and André C Morandini. The puzzling occurrence of the upside-down jellyfish cassiopea (cnidaria: Scyphozoa) along the brazilian coast: a result of several invasion events? *Zoologia (Curitiba)*, 37, 2021.

[19] Elizabeth W Stoner, Craig A Layman, Lauren A Yeager, and Heather M Hassett. Effects of anthropogenic disturbance on the abundance and size of epibenthic jellyfish cassiopea spp. *Marine pollution bulletin*, 62(5):1109–1114, 2011.

[20] Steven Vogel and Michael LaBarbera. Simple flow tanks for research and teaching. *Bioscience*, 28(10):638–643, 1978.